Chapter 5. Numerical Simulation of the Stub Loaded Helix

5.1 Stub Loaded Helix Antenna Performance

The geometry of the Stub Loaded Helix is significantly more complicated than that of the conventional helix antenna. Given the number of parameters that can be adjusted to affect performance, a comprehensive empirical study of the SLH would be a hopelessly daunting task. Fortunately, there are numerical modeling tools available that can be used to predict the performance of this geometry. In Chapter 3, we used simulation results produced by NEC to explore the operation of the conventional axial mode helix. Those results compared favorably with measured and simulated, and theoretical results presented by others, thus validating the use of NEC for conventional helices. We will use NEC again to model the SLH antenna and will validate its use with measured results presented in Chapter 7. In this section, we discuss the numerical models used to simulate the SLH and their results.

5.2 NEC Modeling

The Stub Loaded Helix is a wire antenna. Thus, the obvious choice of modeling techniques is the Method of Moments (MoM) [Stutzman and Thiele, 1981]. In the Method of Moments, the helix geometry is approximated using straight line wires. Each straight line wire is broken into a number of segments. The Method of Moments uses the solution of an integral equation to approximate the currents induced on the wires by sources or incident fields. This method is a highly accurate and versatile tool for electromagnetic analysis.

For the work reported here the Numerical Electromagnetics Code (NEC) [Burke and Poggio, 1981] was used. NEC uses numerical methods to solve the necessary integral equations to find the currents on the wire. Versions of both NEC-2 and NEC-4 were used with comparable results from both.

In creating accurate NEC models of an antenna, there are several guidelines that must be followed. These are the result of some of the approximations and limitations that are inherent in the numerical methods used in the program. Many of these guidelines are well known and detailed in the program documentation. The most common of these is the limitation that the wire segment lengths be longer than the diameter of the wire. This is the "thin wire approximation" and is essential to the form of the kernel used to solve the integral equation that is the basis of the MoM. The NEC models used for the SLH were relatively straightforward, with one exception, which will be detailed below.

A wire grid model of a single circular loop can be constructed using a polygon. The coarseness of the model is a function of the number of side for the polygon. A triangle is an extremely poor approximation to a circle, a square somewhat more reasonable, although still very coarse. A hexagon or octagon are considered good approximations to a circle. Higher order polygons are necessary only if high resolution approximations are required.

The helical winding of the SLH is approximated using an octagonal shape in these studies. The stubs are placed at the vertices of the octagon. The original model of the stub was formed by three straight wire segments in a truncated vee configuration. The angle of the vee formed by the two legs of the stub was typically modeled as 10° to 20°. A short wire truncating the vee is placed at the appropriate distance to make the depth of the stub correct and is modeled by only one wire segment due to its short length.

Initial attempts to model the stubs using two wires in a vee configuration produced spurious results in NEC. It was concluded that if the angle between two wire is too acute, NEC has numerical problems because the volumes of the two wire overlap near the apex of the connection. To avoid this problem, the acute angle was truncated with a third wire. By using a third wire the angle between the two legs of the stubs and the truncating wire is always obtuse. This stub geometry used for NEC modeling is shown in Figure 5.1(a).

While the truncated vee model of the stub produced acceptable results in NEC, it needed to be improved upon. The angle created by the gap added an additional variable to the model that was in practice not consequential in prototype performance.

If made too large, the gap has two deleterious effects on the performance of the NEC models. First, since the legs of the stub were not parallel in this stub model, if the gap is

large enough, the radiation from the stub legs will not cancel. This would most likely show up as a degradation in the axial ratio performance of the antenna. Secondly, an excessive gap width reduces the length of the circumferential wire on the helix. This results in an upward shift in the center operating frequency of the SLH. This effect became evident when comparing simulation results with some of the early prototypes.

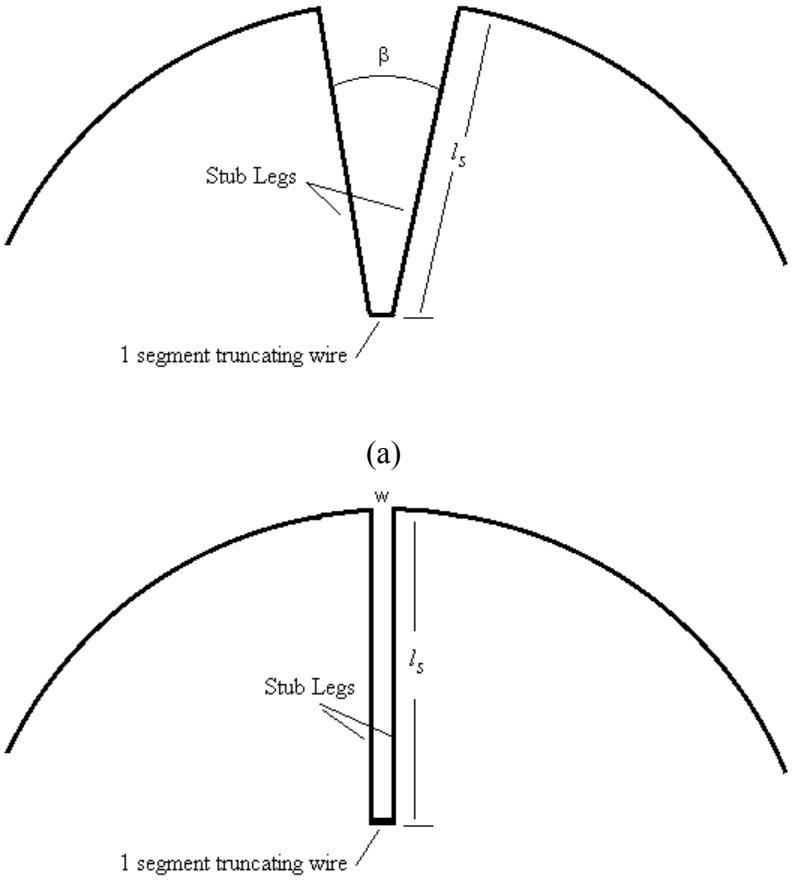

Figure 5.1 Geometry of stubs used for NEC model. (a) Original stub design. Stub legs are joined with a one segment truncating wire to insure there are no acute angles in the stub inner geometry. (b) Improved stub geometry using parallel stub wires.

In order to circumvent these problems, an improved stub model geometry was created. The improved stub model, shown in Figure 5.1(b) consists of two parallel wires that straddle a radial line of the helix circumference and a truncating wire at the stub interior. By using parallel wires, maximum cancellation of the stub radiation occurs. It is still

important to minimize the stub width, w, but the use of parallel wire makes this easier from a geometric modeling viewpoint. It is known that care must be taken in NEC when modeling closely spaced parallel wires. However, as long as the wires are of equal diameter, their spacing exceeds several wire diameters, and the segmentation of the wires is identical, NEC can handle these closely spaced wires.

In all of the NEC simulations, in this chapter and others, no attempt was made to impedance match the helix to the feed of the antenna. The feed consists of a vertical wire from the lower end of the helix to the underlying groundplane. A simple NEC voltage source feed is placed in the middle of this vertical wire to simulate the actual source. The result is that the gain simulation results do not include any mismatch losses. Thus they are not realized gain numbers. The feed model does not effect the pattern or axial ratio results predicted by NEC. The measured results presented later all included a matching section to provide a VSWR of less than 2:1 in a 50 Ω system, thus their gains are realized gains that include a small amount of mismatch loss.

In the following sections detailed results of several NEC models for various SLH designs will be presented. Table 5.1 summarizes those models for convenience. The UHF models are used to get an overall sense of the performance behavior and characteristics of the SLH antenna. These are used as the baseline models for the parameter studies presented in Chapter 6. The S-band models presented will be used as the basis for the verification and evaluation of the modeling results as they reflect experimental prototypes whose results are presented in Chapter 7.

Table 5.1 Summary of NEC Models and Descriptions

Description	Model ID
5-turn UHF SLH, infinite groundplane	M5-1
5-turn UHF SLH, wiregrid groundplane	M5-2
10-turn UHF SLH, infinite groundplane	M10-1
10-turn UHF SLH, wiregrid groundplane	M10-2
10-turn S-band SLH, infinite groundplane	M10-3
15-turn S-band SLH, infinite groundplane	M15-1

5.3 Simulation of a Five Turn SLH (M5-1,2)

A numerical study of the Stub Loaded Helix geometry was conducted using NEC4 to model a basic SLH antenna. The reference model, whose design parameters are shown in Table 5.2, consisted of a 5-turn SLH antenna with a circumference of 1 m. The reference model had four stubs/turn, with a depth of 0.1061 m (0.6666·R). The first model, M5-1, was of an SLH fed against an infinite groundplane. A second model, M5-2, was constructed with a 2.4 m by 2.4 m wiregrid groundplane replacing the infinite groundplane of the first model. The groundplane consisted of a rectangular grid of wires with a spacing between wires of 0.1 m. In both models the helix was elevated 0.03 m above the groundplane. The frequency range of the simulation covered 175 to 275 MHz.

Table 5.2 Design parameters of 5-turn reference SLH (M5-1,2)

C, circumference	1 m
R, radius	15.9 cm
D, diameter	31.8 cm
α, pitch angle	8°
S, turn-to-turn spacing	14 cm
N_s, stubs/turn	4
l_s. stub depth	10.6 cm
N, # turns	5
f_c, nom. center frequency	235 MHz

Figure 5.2 shows predicted patterns for the infinite groundplane model. The patterns only cover the forward hemisphere due to the presence of the infinite groundplane. All the patterns are essentially similar with only a slight variation in gain with frequency.

Figure 5.3 shows predicted patterns for the wire grid groundplane model. These are full 360° patterns showing side- and back lobes. The predicted gains are slightly higher than for the infinite groundplane cases. The front-to-back ratio is at least 20 dB except at the lowest frequency.

Figure 5.4 shows the predicted boresight gain for the five turn SLH modeled with both the infinite and the wiregrid groundplanes. As noted previously, the wiregrid groundplane exhibits a slightly higher gain than the infinite groundplane results. The gain of both models is relatively flat with frequency with a slight increasing gain trend with frequency.

Figure 5.5 shows the predicted boresight axial ratio with frequency for both infinite and wiregrid groundplane models. Both models exhibit the same trend with frequency and similar peak axial ratios, but the curve for the wiregrid groundplane model is shifted down slightly from the infinite groundplane curve by approximately 2% in frequency. Both models exhibit a rapid deterioration of axial ratio at the upper frequency end of the curve after passing through a peak. This is a characteristic of the Stub Loaded Helix performance. A reference line is included at the 3 dB level to indicate what is typically considered the useable axial ratio bandwidth of the antenna.

Many applications specify a maximum axial ratio of 3 dB for antenna performance. An axial ratio of 3 dB translates into a maximum system loss of 0.50 dB [Ludwig, 1976]. This assumes a 3 dB axial ratio at both ends of the communications link and maximum misalignment of the antennas in polarization. In applications such as satellite communications where link margin is a precious commodity, such stringent requirements are necessary. Axial ratios much greater than 3 dB are tolerable in applications, such as terrestrial communications, where link margins are usually not as critical.

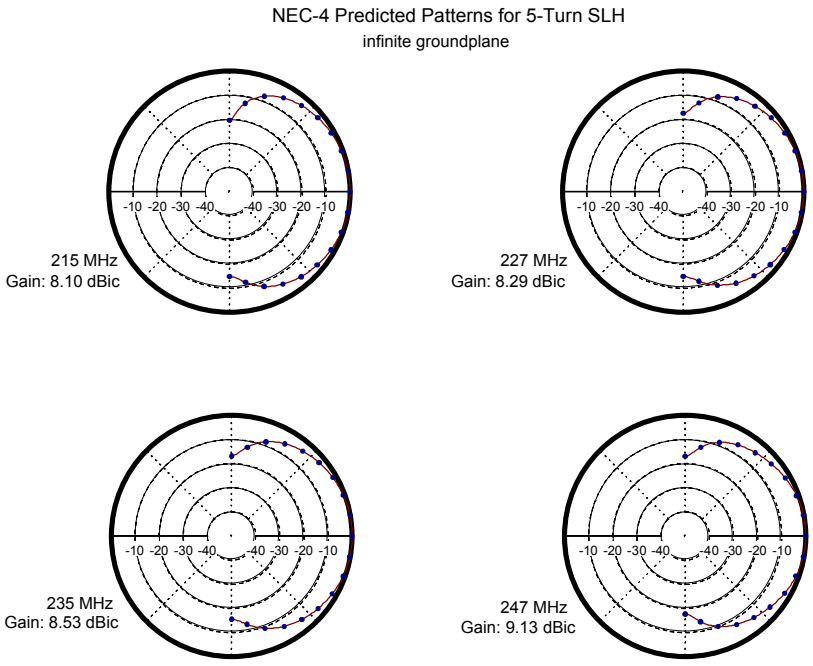

Figure 5.2 NEC-4 predicted patterns of five turn SLH in Table 5.2 over an infinite groundplane, model M5-1.

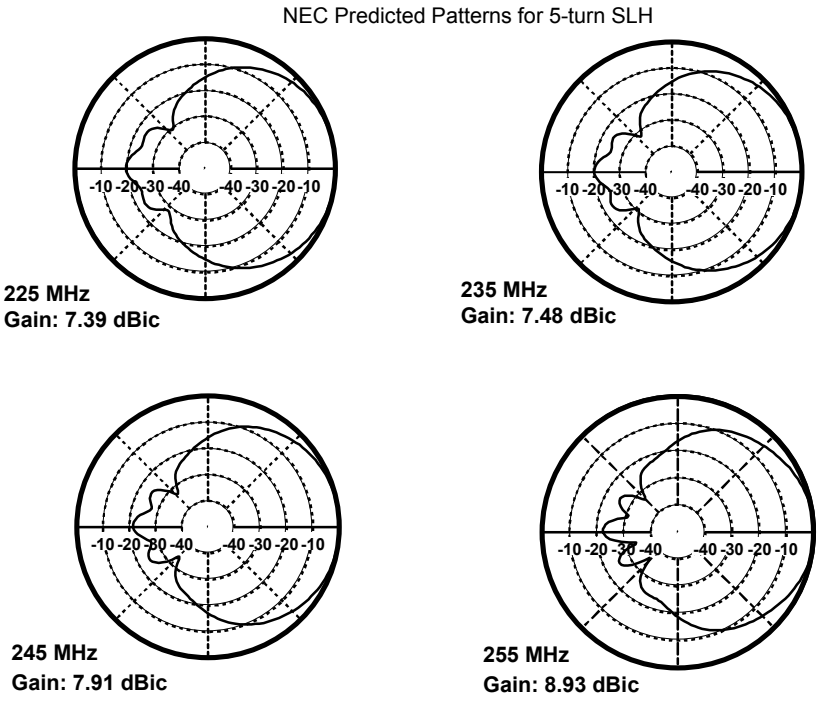

Figure 5.3 NEC-4 predicted patterns of five turn SLH in Table 5.2 over a 2.4 m x 2.4 m wiregrid groundplane, model M5-2.

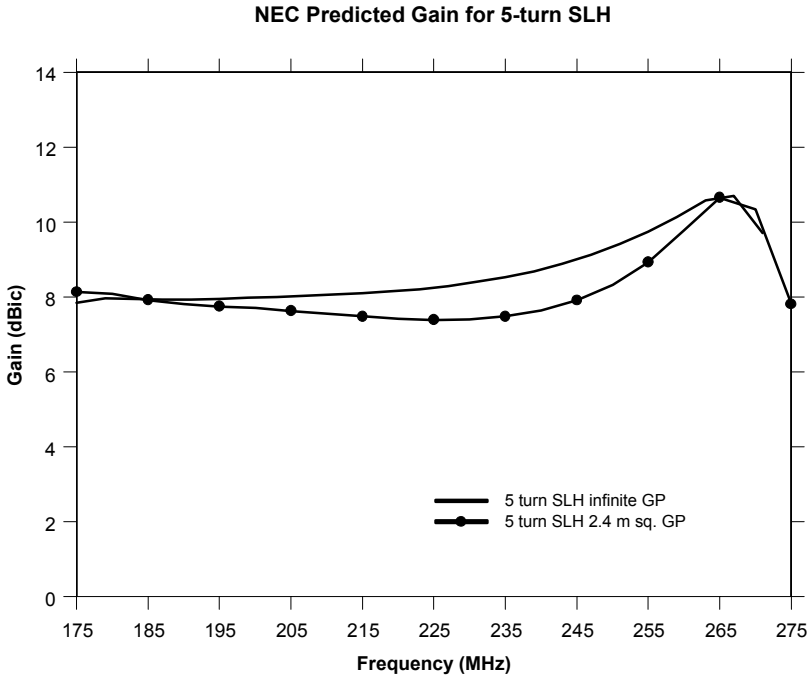

Figure 5.4 NEC-4 predicted gain for the five turn SLH in Table 5.2 over infinite ground and a 2.4 m x 2.4 m wiregrid groundplane (M5-1,2).

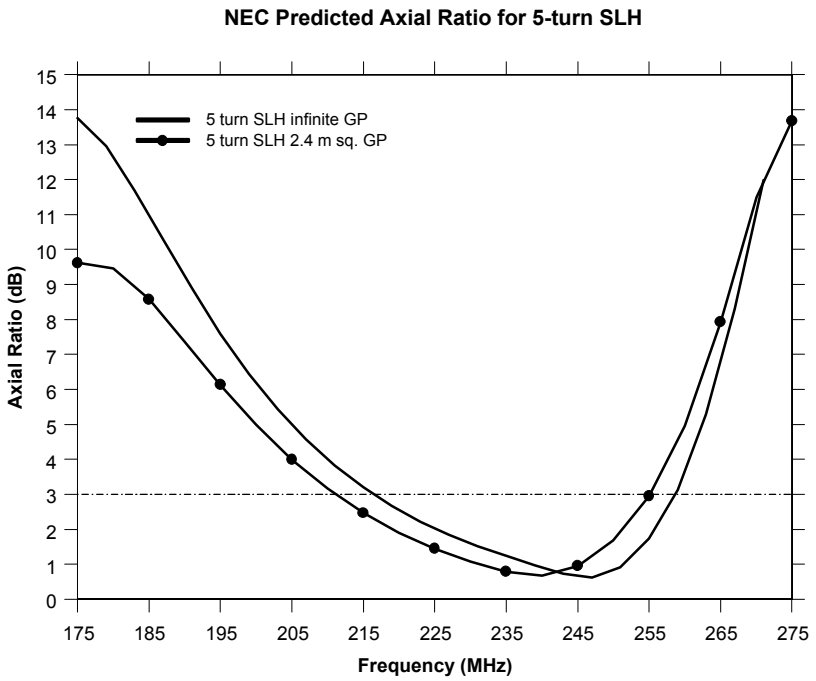

Figure 5.5 NEC-4 predicted axial ratio for the five turn SLH in Table 5.2 over infinite ground and a 2.4 m x 2.4 m wiregrid groundplane (M5-1,2).

If we assume that the axial ratio is the performance limiting factor for the SLH, as is suggested by Figure 5.5, the model results indicate that the operational bandwidth of the 5-turn SLH modeled here is from 210 MHz ($f_L = 0.89\ f_c$) to 260 MHz ($f_u = 1.10\ f_c$), which corresponds to a center frequency of 235 MHz (f_c) and a bandwidth of 21%. A conventional axial mode helix with the same circumference would have a nominal center frequency of 300 MHz. The SLH modeled here has a center frequency 0.78, or 22% lower than, the full size helix.

5.4 Simulation of a Ten Turn SLH (M10-1,2)

For comparison, a ten turn Stub Loaded Helix with identical parameters to the five turn SLH in the previous section was modeled. The design parameters are identical to those in Table 5.2 except that ten turns were used instead of five. It too was modeled over both an infinite groundplane (M10-1) and a 2.4 m x 2.4 m wiregrid groundplane (M10-2). Patterns for the infinite groundplane are shown in Figure 5.6. The two highest frequency

patterns show the formation of sidelobes at approximately ±80°, a feature missing from the five turn SLH patterns.

Figure 5.7 shows the predicted patterns with the 2.4 m x 2.4 m wiregrid groundplane. Once again, the gain of the wiregrid groundplane models is slightly higher than the infinite groundplane models. The sidelobe structure visible in the infinite groundplane models is also visible here but has a lower level and is also at a great angle than in the infinite groundplane models. The backlobe structure is symmetric and shows a front-to-back ratio greater than 15 dB across the band examined.

Figure 5.8 shows the computed boresight gain for infinite and wiregrid groundplane models. The gains for both are relatively flat across most of the frequency range modeled and within approximately 0.5 dB of each other. Both models shows a sharp gain dip at approximately 179 MHz. This gain dip has also been observed in experimental data, so it may not be a modeling anomaly. We have no ready explanation for this. Both curves show a dramatic gain rolloff above 250 MHz. This sharp gain rolloff appears to be characteristic of the Stub Loaded Helix. It is also slightly visible at the upper frequency end in the five turn SLH modeling results in Figure 5.4.

Figure 5.9 shows the predicted axial ratio results for the ten turn models. Unlike the five turn SLH results, there is not a frequency shift between the infinite groundplane and wiregrid groundplane results. Both models exhibit approximately the same axial ratio performance. The shape of the axial ratio curves are more symmetric than in the five turn SLH model results. This can be attributed to the longer length of the ten turn antenna.

The axial ratio on a helix antenna is determined in large part by the interaction of the forward directed T1 mode traveling wave and the reverse directed (reflected) T1 mode traveling wave on the helix. Assuming the helix structure is ideal, if only the forward directed T1 mode traveling wave existed, pure circular polarization would be generated. The reverse directed T1 mode wave is created by a reflection of the forward directed traveling at the end of the helical winding. This wave has the opposite sense of polarization and its radiation degrades the purity of the (correct sense) circular polarization. The longer the helical winding, the greater the attenuation of the forward traveling wave before it is reflected at the end. Thus, it is expected that a longer helix will have better axial ratio performance than a shorter one.

Again, if we assume the axial ratio value of 3 dB is the specification, then AR becomes the bandwidth limitation in most cases of the SLH. From Figure 5.9, the center frequency of the ten turn SLH is 225 MHz and the bandwidth is 50 MHz, or 22.2%. This is a center frequency reduction of 0.75, or 25% lower than, a full size helix of the same diameter.

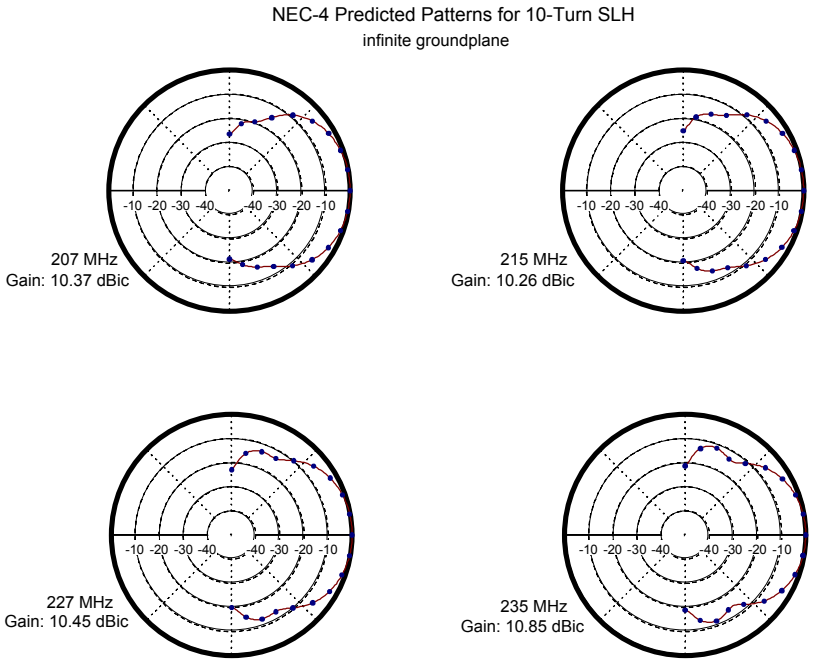

Figure 5.6 NEC-4 predicted patterns of ten turn SLH over an infinite groundplane (M10-1). Helix design parameters of Table 5.2 except for N=10.

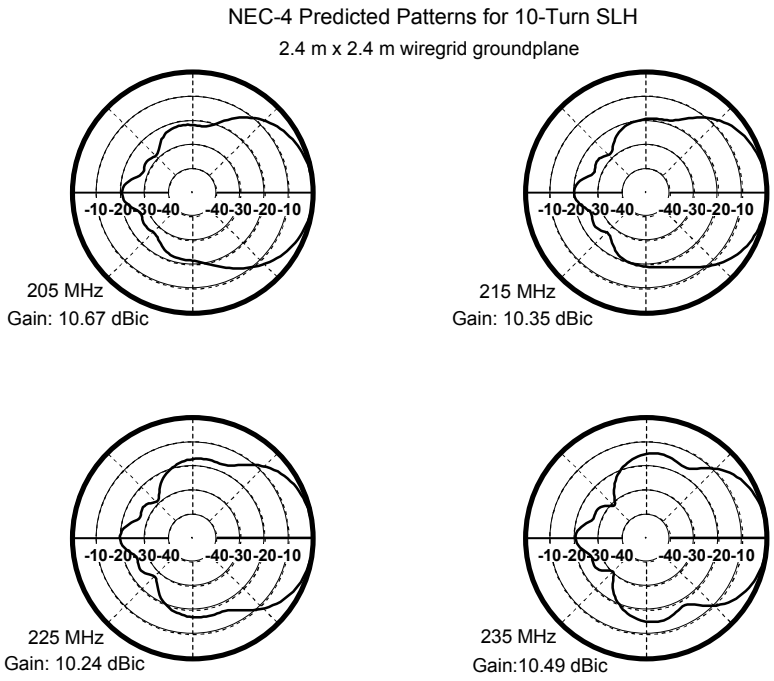

Figure 5.7 NEC-4 predicted patterns of ten turn SLH over a 2.4 m x 2.4 m wiregrid groundplane (M10-2). Helix design parameters of Table 5.2 except for N=10.

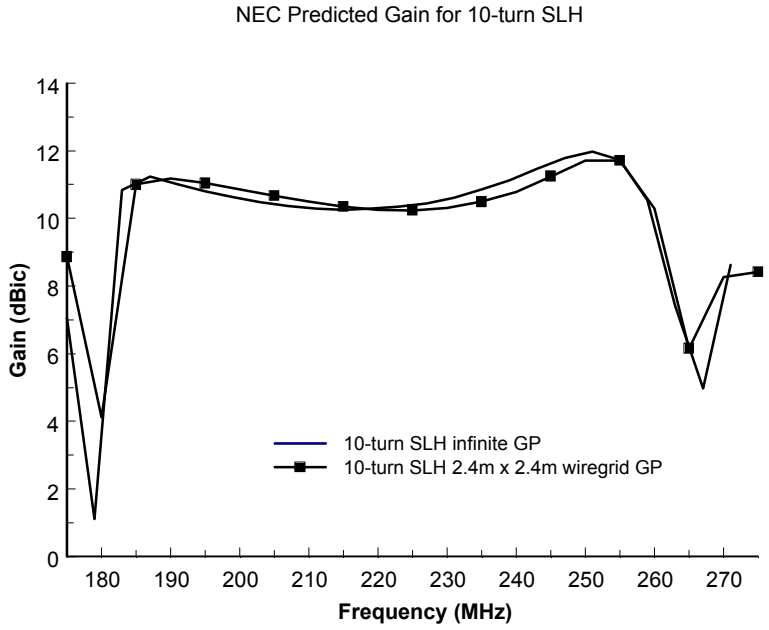

Figure 5.8 NEC-4 predicted gain for a ten turn SLH over infinite ground (M10-1) and a 2.4 m x 2.4 m wiregrid groundplane (M10-2). Helix design parameters of Table 5.2 except for N=10.

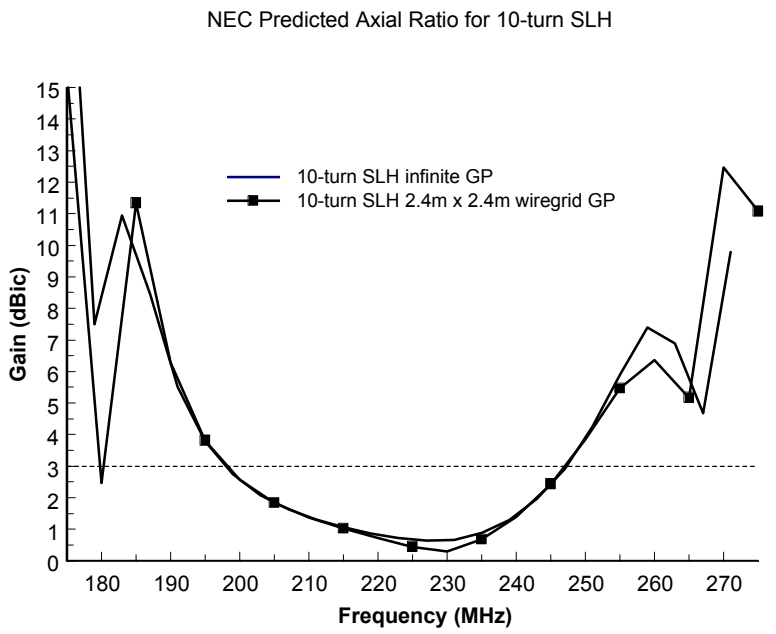

Figure 5.9 NEC-4 predicted axial ratio for a 10-turn SLH over infinite ground (M10-1) and a 2.4 m x 2.4 m wiregrid groundplane (M10-2). Helix design parameters of Table 5.2 except for N=10.

5.5 10-turn S-band SLH (M10-3)

The previous models provided a good overview of the performance we should expect from an SLH antenna. The dimensions used in those models are, however, too large to feasibly construct and measure on our antenna ranges. In Chapter 7 we present the measured results of several prototype SLH antennas that were built for use in the region of 2.4 GHz. At this frequency the antenna dimensions are small enough to be easily constructed and our antenna ranges can measure their gain and patterns.

In order to compare the results of our modeling with the measured results in Chapter 7, we present two models, one in this Section and one in the next, that approximate two of the prototypes measured.

The design parameters for the first prototype model are given Table 5.3. It is a 10-turn SLH for S-band and is designated as model M10-3. Figure 5.10 shows the gain and axial ratio performance of this antenna as predicted by NEC.

Table 5.3 Design parameters of 10-turn S-band SLH (M10-3)

C, circumference	7.979 cm
R, radius	1.27 cm
D, diameter	2.54 cm
α, pitch angle	8°
S, turn-to-turn spacing	1.121 cm
N_s, stubs/turn	4
l_s. stub depth	8.458 mm
N, # turns	10
f_c, nom. center frequency	2.5 GHz

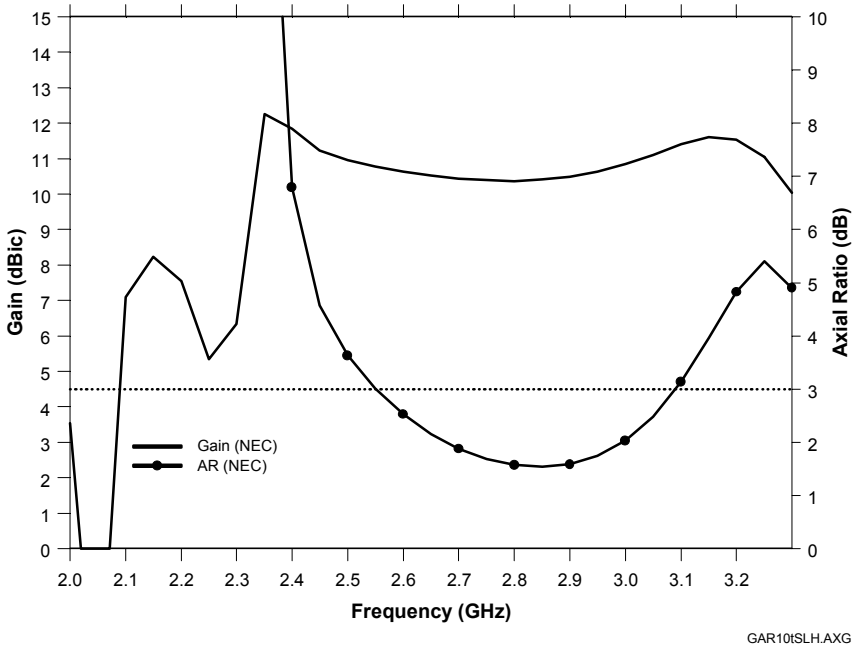

Figure 5.10 NEC predicted gain and axial ratio of 10-turn S-band SLH over infinite groundplane (M10-3). Helix design parameters given in Table 5.3.

Based on the NEC results, the center frequency is 2.81 GHz and the 3-dB axial ratio bandwidth is 530 MHz (18.8%). Over the usable operating bandwidth the gain varies between 10.3 and 11.1 dBic.

Although the center frequency is higher than desired, the basic shape of the gain and axial ratio curves are similar to those observed in the previous models. These results will be utilized later to compare to measured results.

5.6 15-turn S-band SLH (M15-1)

The second model of an experimental prototype is a 15-turn S-band SLH with the same design parameters as in Table 5.3, except for the number of turns, N. This model was designated M15-1.

Figure 5.11 shows the NEC predicted gain and axial ratio performance of this model. The usable operating bandwidth, as determined by the 3 dB axial ratio bandwidth, is 700 MHz with a center frequency of 2.80 GHz. This corresponds to a percentage bandwidth of 25%. Again, it is noted that the center frequency is slightly higher than intended based on the design parameters in Table 5.3. Over the usable bandwidth the gain varies from 11.4 to 13.0 dBic. These results will be used later to compare to measured data from an experimental prototype.

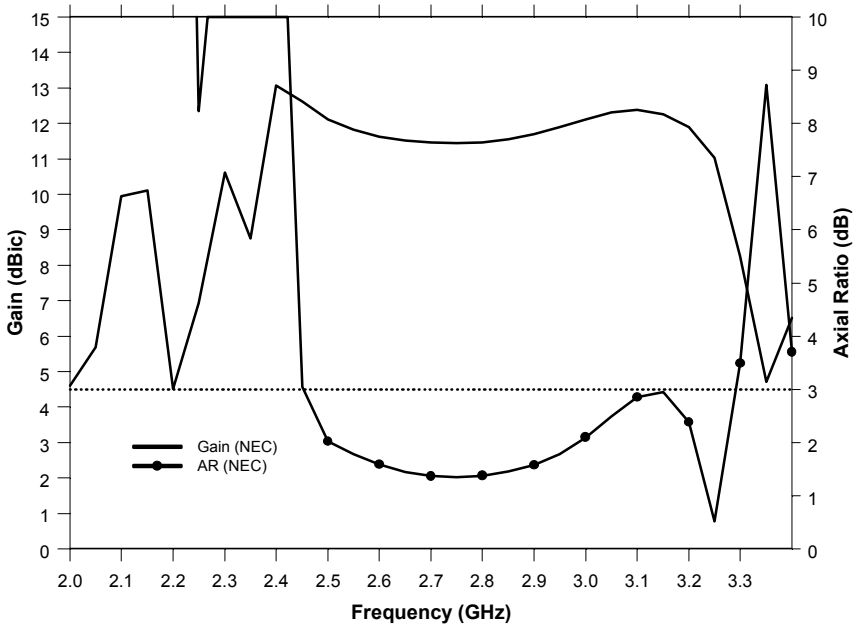

Figure 5.11 NEC predicted gain and axial ratio of 15-turn S-band SLH over infinite groundplane (M15-1). Helix design parameters same as Table 5.3 except N=15.

5.7 Summary of Model Results

In the previous sections we have presented NEC modeling results for several different designs of SLH antennas. The first four models (M5-1,2 and M10-1,2) used a nominal 1 m circumference to enable an easy understanding of the size reduction performance of the SLH as well as presenting representative performance characteristics. They were also used to examine the differences between models that assumed an infinite groundplane and those with a finite wiregrid groundplane, which is more representative of real world antennas.

The second group of models (M10-3 and M15-1) were designed to closely approximate the physical dimensions of experimental prototypes that were built and measured. Comparisons of the results between modeling and experiments will be presented in Chapter 8.

Table 5.4 presents a summary of the performance results for all the models presented in this chapter. The center frequency, f_c, is based on the 3-dB axial ratio bandwidth of the antennas, as is the bandwidth, BW, and percentage bandwidth shown in Table 5.4. The third column in Table 5.4, labeled % $f_{c_{fs}}$, shows the percentage of reduction of the predicted center frequency of the SLH from the center frequency of a full size conventional helix with the same circumference. The maximum and minimum gains, G_{max} and G_{min}, correspond to the maximum and minimum gains across the 3-dB axial ratio bandwidth, respectively.

Table 5.4 Summary of Model Performance Parameters

Model	f_c	% $f_{c_{fs}}$	BW (3 dB AR)	% BW	G_{max} (dBic)	G_{min} (dBic)
M5-1	237.5 MHz	79.1	41 MHz	17.2	10.0	8.1
M5-2	233.0 MHz	77.6	43 MHz	18.4	8.93	7.39
M10-1	223.0 MHz	77.6	50 MHz	22.4	11.8	10.2
M10-2	222.0 MHz	74.0	50 MHz	22.5	11.2	10.2
M10-3	2.81 GHz	74.7	530 MHz	18.8	11.1	10.3
M15-1	2.80 GHz	74.5	700 MHz	25.0	13.0	11.4

In conclusion, the preceding simulations of the 5- and 10-turn SLH (M5-1,2 and M10-1,2) indicate that the center frequency of an SLH antenna is approximately 22-25% lower than

that of a conventional helix of the same diameter. The axial length of the SLH is approximately 50% or less of that of the corresponding conventional helix with the same number of turns. These lead to a dramatic volume reduction of at least 70%.

The usable bandwidth of the SLH, as determined from its 3 dB axial ratio bandwidth, is approximately 22% of the center frequency of operation. Conventional helices can have bandwidths of 50%. But the 22% bandwidth typical of the SLH is more than adequate for many applications.